Taylor & Francis
Taylor & Francis Group

Artificial Cells, Nanomedicine, and Biotechnology

An International Journal

ISSN: 2169-1401 (Print) 2169-141X (Online) Journal homepage: https://www.tandfonline.com/loi/ianb20

Investigating the effect of near infrared photo thermal therapy folic acid conjugated gold nano shell on melanoma cancer cell line A375

Fateme Sadat Majidi, Elham Mohammadi, Bita Mehravi, Samira Nouri, Khadije Ashtari & Ali Neshasteh-riz

To cite this article: Fateme Sadat Majidi, Elham Mohammadi, Bita Mehravi, Samira Nouri, Khadije Ashtari & Ali Neshasteh-riz (2019) Investigating the effect of near infrared photo thermal therapy folic acid conjugated gold nano shell on melanoma cancer cell line A375, Artificial Cells, Nanomedicine, and Biotechnology, 47:1, 2161-2170, DOI: 10.1080/21691401.2019.1593188

To link to this article: https://doi.org/10.1080/21691401.2019.1593188

Published online: 03 Jun 2019.

ARTIFICIAL CELLS, NANOMEDICINE, AND BIOTECHNOLOGY
2019, VOL. 47, NO. 1, 2161–2170
https://doi.org/10.1080/21691401.2019.1593188

Investigating the effect of near infrared photo thermal therapy folic acid conjugated gold nano shell on melanoma cancer cell line A375

Fateme Sadat Majidi[a,c], Elham Mohammadi[b], Bita Mehravi[b], Samira Nouri[a,c], Khadije Ashtari[b] and Ali Neshasteh-riz [a]

[a]Radiation Biology Research Center, Iran University of Medical Sciences, Tehran, Iran; [b]Department of Medical Nanotechnology, Faculty of Medical Nanotechnologies, University of Medical Sciences, Tehran, Iran; [c]Cellular and Molecular Research Center, Iran University of Medical Sciences, Tehran, Iran

ABSTRACT

Nowadays, there is growing interest regarding the use of metal Nanoshells as targeted agents of Nano-photo thermal cancer therapy. This study was aimed at synthesis the folic acid (FA)-conjugated with silica @gold core-shell nanoparticles (FA-SiO_2@AuNPs) for improving the treatment of melanoma cancer cells. The characterization data showed that the FA-SiO_2@AuNPs is spherical in shape and its size is ~73.7 nm. The intracellular uptake of FA-SiO_2@AuNPs into melanoma cells (A375**)** was measured through the inductively coupled plasma, (~47.7%). The cytotoxicity of nanoparticles was investigated on A375 and HDF (Human dermal fibroblast) cell lines. Cytotoxicity results indicated that there is no significant cytotoxicity in HDF cell lines treated with nanoparticles. MTT and flow cytometry results showed that the viability of A375 cells treated by SiO_2@Au and FA-SiO_2@AuNPs was decreased significantly to about 31% and 16% respectively. The higher toxicity of cancer cells was obtained for the cells exposed to 808 nm near-infrared (NIR) laser after incubation with FA-SiO_2@AuNPs rather than the non-targeted SiO_2@AuNPs. Furthermore, about 64% more cell death was observed for A-375 cells using both photothermal therapy and treatment with FA-SiO_2@AuNPs compared to photothermal therapy. Additionally, the majority of the cell deaths were related to the apoptosis process, not necrosis. It can be concluded that FA-SiO_2@AuNPs was an effective targeting agent for photothermal therapy in the treatment of melanoma.

ARTICLE HISTORY
Received 1 December 2018
Revised 31 January 2019
Accepted 31 January 2019

KEYWORDS
Folic acid; gold shell; hyperthermia; melanoma cancer; nanoparticle

Introduction

Malignant melanoma, as the major fatal form of skin cancer, is an aggressive cancer derived from melanocytes [1]. In recent years, the incidence of melanoma has been increasing continuously worldwide [2]. In 2016, it is estimated that 73,670 new cases of melanoma will be diagnosed in the USA only and about 9940 numbers regarding mortality rate will be reported [3,4].

Presently, there are several methods for the treatment of melanoma cancer. Surgery, radiation therapy, and chemotherapy are the standard methods for treating melanoma [5,6]. The disease is curable intrinsically, although it depends on early diagnosis [7]. Late stage melanoma is not curable by current clinical tools. Despite the recent technological advancements in these methods, the need for an efficient method for melanoma cancer therapy still remains [8].

Therefore, several novel nanotechnology-based methods for cancer diagnosis and therapy are under investigation [9–11]. Gold nanoparticles have represented a completely new technology in the field of photothermal therapy (PTT), which have been favored considerably in recent years [11,12]. Several methods, including microwave irradiation [13], RF pulses [14], and ultrasound [15] have been used for the delivery of thermal energy to cancer tissue.

The commonly utilized gold nanoparticles for cancer therapy include gold Nano spheres [16], Nano shells [17], Nano rods [18] and Nano cages [19] Depending on the shape and size, gold nanoparticles can absorb and scatter light in the visible and NIR wavelength regions [20].

Table 1 summarizes recent *in vitro* studies on various nanoparticles and compares the percentage of cell death induced by laser exposure to cancer cells [18,23].

The photothermal properties of AuNPs indicate that if AuNPs enter cancerous cells, they will cause photothermal effects after irradiating by a light source. Therefore, it is necessary to design AuNPs such that they can target cancerous cells selectively. This characteristic of AuNPs has been investigated for improving photothermal therapy cancer treatment [25]. The specific targeting of these nanoparticles to cancer cells could increase the cancer cell death by NIR laser [26]. As a result, folic acid (folate) was used as a targeting agent, which was conjugated to SiO_2@Au [23,27].

CONTACT Bita Mehravi Mehravi.b@iums.ac.ir Department of Medical Nanotechnology, Iran University of Medical Sciences, Tehran 1449614535, Iran; Ali Neshasteh-riz neshastehriz.a@iums.ac.ir Radiation Biology Research Center, Iran University of Medical Sciences, Tehran 1449614535, Iran

Table 1. Summary of *in vitro* studies on nanoparticles.

Reference	Cell Line, Origin	Nanoparticle; Size (nm)	Nanoparticle Concentration [μg/ml]	Exposure Conditions [nm; W/cm^2; Sec]	Cell death%
Wang et al. [11]	KB, Nasopharynx	FA-Fe_3O_4@GNR[1] 90 nm	100	808; 10; 4	>50
Eyvazzadeh et al. [21]	KB, Nasopharynx	Au@IONPs[2] 33 nm	50	808; 6; 5	>45
Ghaznavi et al. [22]	KB, Nasopharynx	FA-Fe_3O_4@Au[3] 60nm	50	808; 6; 10	38
Mansoori et al. [23]	HeLa, Cervix	Folate-MH[4]-Au; 40	20	560; 250; .06	75
Kristine. [24]	PC3 Prostate	$K_{60}L_{20}$ [4]vesicles with gold 100–200 nm	NI	808; .2; 10	NI

1Superparamagnetic iron oxide (SPIO) core and gold Nano rod (GNRs) in the mesoporous silica shell functionalized with folic acid. [2]Gold@ iron oxide nanoparticles. [3]Mercapto-Hexanole. [4]Poly (L-lysine)$_{60}$-block-poly(L-leucine)$_{20}$. [nm; W/cm^2; Sec] represents[nanometer; power density; exposure time]. "NI" represents Not Informed.

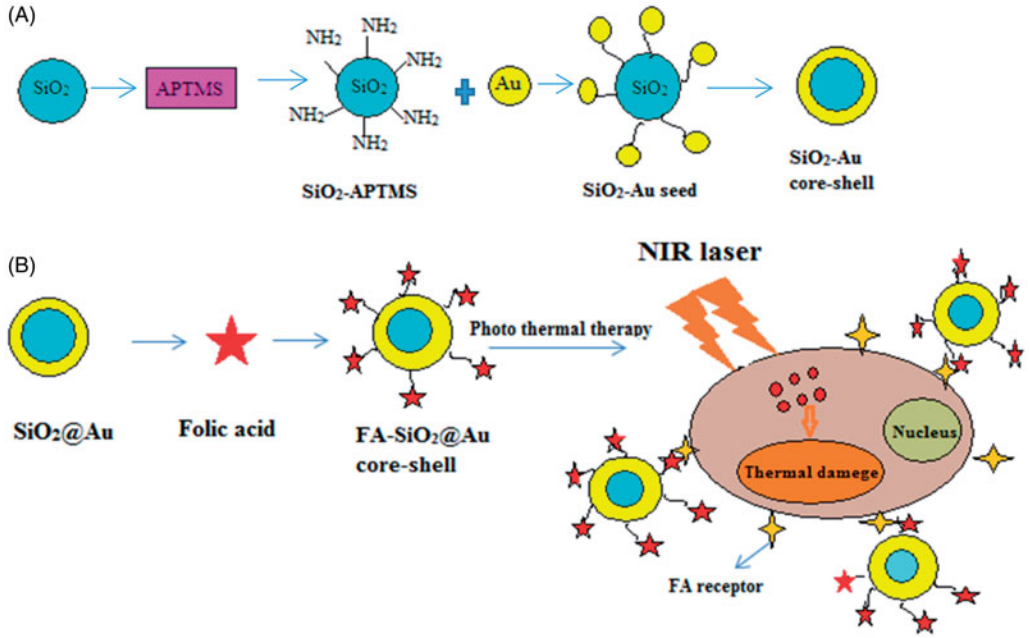

Scheme 1. A schematic description for synthesis SiO_2@Au and FA-SiO_2 @AuNPs (A) and photo thermal ablation of melanoma cells under NIR laser irradiation (B).

Folic acid is one of the substances, which can be applied as targeting agents for therapeutic methods [28]. Folic acid as one of the small molecules is a water-soluble vitamin of the B-complex group, which is essential for cell division and growth. Almost all cells express the folate receptor, but cancer cells tend to overexpress the folate-receptor due to their great requirement to folate to provide energy due to the high rate of cell division and proliferation [29,30]. Folic acid is applied as an appropriate targeting agent, which is also utilized in this study.

In this study, a nanoparticle was designed. SiO_2@AuNPs is a new type of nanoparticles composed of a dielectric silica core coated with a thin layer of gold. Silica core was synthesized and gold was coated on the surface of silica core, then Folic acid was functionalized on SiO_2@AuNPs. The synthesized FA-SiO_2@AuNPs was characterized by Dynamic Light Scattering (DLS) and Scanning Electron Microscopy (SEM), Fourier transform infrared microscopy (FTIR), UV-visible spectroscopy (UV visible). FA-SiO_2@AuNPs had a high uptake in the cancer cells of melanoma and induced more death in cancer cells compared to normal cells induced by NIR laser irradiation. In this study, after the preparation of FA-SiO_2@AuNPs, the effects of the photothermal therapy of these nanoparticles on A375 cell line were assessed. In order to assess the results, MTT assay and flow cytometry were performed. Scheme 1 illustrates the theme of the current study in brief.

Materials and methods

Chemical material

Hydrogen tetrachloroaurate (III) ($HAuC_{l4}$, $3H_2O$, 99.99%, Alfa Aesar), sodium hydroxide (NaOH, Sigma-Aldrich), potassium carbonate (K_2CO_3, AR Grade) and sodium borohydride ($NaBH_4$, Aldrich) amino propyltriethoxysilane (APTES, 99%), tetraethyl orthosilicate (TEOS, 98%), anhydrous ethanol (EtOH, 99.5%), were provided from Acros Co. (Belgium) and were used without further purification. Using 500–1000 Da cut off was obtained from the Spectrum Lab (USA). Dimethyl Sulphoxide (DMSO), Dicyclohexyl Carbodiimide (DCC), Folic acid, Dichloromethane (CH_2Cl_2), Fetal bovine serum (FBS), penicillin sterptomycine and Dulbecco's modified Eagle's medium (DMEM), 3-[4, 5-dimethyl thiazol-2-yl]-2, 5-diphenyl

tetrazolium bromide (MTT), Annexin V-FITC and propidine Iodide (PI) were purchased from Sigma Aldrich (Germany). Human Dermal Fibroblast cell lines (HDF) and A375 cell lines were provided from National Cell Bank of Pasteur Institute of Iran.

Instrumentation

The Au ions were quantified using an inductively coupled plasma mass spectrometry (ICP-mass, JY138 Spectro -analyzer; Horiba Jobin Yvon, Inc., Edison, NJ). The data were analyzed using Coulter software. The absorbance was measured at 450 nm by a BioTek's absorbance micro plate readers (ELX800, Biotek, USA). SEM (Philips 97, XL-30, Holland). DLS (Nano flex zeta sizer, Germany). FTIR (spectrophotometer, Perkin Elimer, Frontier, USA (UV-visible spectrophotometer, Pharmacia Biotech, Germany). MTT (microplate reader Bio-rad,). Flow cytometry (BDbiocsiences, SanJose, CA, USA).

Synthesis of monodispersed silica (nanoparticle)

Silica nanoparticles were prepared with an average diameter of ~73.7 nm by hydrolysis of tetraethylortho silicate (TEOS) in ethanol medium with the presence of deionized water and ammonium hydroxide according to the study by Stöber et al [31]. Briefly, a solution of TEOS: EtOH: H_2O: NH_4OH (1.0:10.0:1.0:8 ml) was stirred vigorously for 30 min to obtain a white turbid suspension. The nanoparticles were separated by centrifugation (12,000 rpm, 12 min). Ultimately, the product was washed using 5 cc deionized water and ethanol twice.

Preparation of APTES-grafted silica

Amino propyltriethoxysilane (APTES) was added to the silica nanoparticle at a 2.0:1.0 weight ratio of APTES: silica was stirred for 24 h at room Temperature. The product was collected by centrifugation (12,000 rpm, 12 min), after which it was washed by deionized water and ethanol twice [32].

Gold seeding on APTES-grafted silica

The APTES-grafted silica nanoparticles were seeded with gold at pH = 7 by adding 2.0 ml of 0.1 M NaOH in 10 ml of the gold stock solution to 2 ml of dispersed silica. The suspension was stirred for 30 min. The product was separated by centrifugation (12,000 rpm/15 min) and it was washed by deionized water and ethanol twice [32].

Synthesis of silica @gold core-shell

Gold-K solution Potassium (gold-K) was synthesized by mixing aqueous K_2CO_3 (280 mg/l) solution with of $HAuCl_4$ (25 mM) stock solution under continuous stirring in the dark for 1 h. Gold Nanoshells were prepared by mixing the Au-K: $AuCl_4$-seeded silica volume at the ratios of 100:1 using 0.01 M $NaBH_4$ as the reducing agent [30,31].

Conjugating folic acid on gold nanoshells

In order to prepare functionalized nanoparticle with folate, 0.1 g of Folic acid was dissolved in 10 ml of Dimethyl Sulphoxide (DMSO) as a solvent and 0.06 g of (N, N′-Dicyclohexyl carbodiimide (DCC) was added for activating the Carboxyl group of Folic acid. Then, the mixture solution was added to 10 ml of CH_2Cl_2, which was exposed to ultrasound for 20 min. Then the solution was stirred for 24 h at room temperature. After 24 h, the mixed solution was purified by centrifuge and was washed 3 times by deionized water and ethanol. The synthesis procedures of SiO_2@AuNPs and FA-SiO_2@AuNPs are illustrated in Figure 1.

Cell culture

Human malignant melanoma A375 cell line and Human dermal fibroblast (HDF) were maintained in Dulbecco's modified Eagle's medium (DMEM), supplemented with 10% fetal bovine serum and 1% of penesterep. A375 and HDF are adherent cell lines and were maintained as a monolayer.

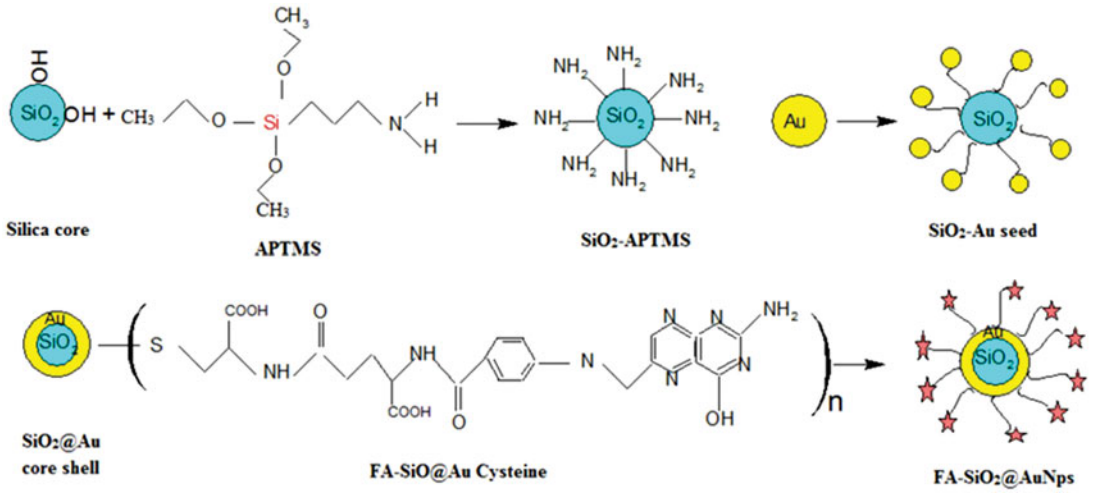

Figure 1. Schematic illustration of synthesis procedure of SiO_2@Au and FA-SiO_2@AuNPs.

Both cell lines were maintained under physiological conditions in an incubator (37 °C, 5% CO_2 and 95% humidity).

Intra-cellular uptake of folic acid gold nanoshell

For detecting intra-cellular uptake of FA-SiO_2@AuNPs, A375 cells were re-plated into 6-well plates at a concentration of 1×10^5 cells per well and were incubated at 37 °C and 5% CO_2 for 24 h. FA-SiO_2@AuNPs (100 μg/ml) was added to each well (1 ml media). Cells were incubated at 37 °C and 5% CO_2 for 2 h, was washed twice by PBS (500 μl) to remove free nanoparticles, then the cells were detached by Trypsin/EDTA resuspended in 1 ml PBS and it was centrifuged at 1000 rpm for 4 min. After removal of the supernatant, the cells were re-suspended in PBS, cells density and viability were determined through staining with trypan blue and counting cells using a hemocytometer. The intracellular uptake of Au ions was determined by ICP-mass, quantitatively. The measurements were performed in triplicate and the mean ± SD of the results were calculated.

Cytotoxicity assays

The cytotoxicity of SiO_2@Au and FA-SiO_2@AuNp on A375 and HDF cell lines was measured by MTT assay. Cells were seeded in 96-well plates at a density of 1×10^4 for A375 and HDF at a density of 2×10^4 cells per well. Afterwards, cells were treated by different concentration of (6.25, 12.5, 25, 50, 100, 200, 400 μg/ml) Nanoparticles added in DMEM with 10% FBS. After 24 h of treatment, the effect of Nanoparticles on cell viability was assessed by the MTT assay. Briefly, after adding 100 μl of MTT (0.5 mg/ml) to each well, the mixtures were incubated for 4 h at 37 °C. The supernatant was aspirated, and the MTT-formazan crystals were formed by metabolically viable cells and were dissolved in 100 μl of DMSO under 15 min incubation. Finally, the absorbance was measured by a microplate reader at a wavelength of 570 nm. The relative cell viability was calculated compared to control wells containing medium without nanoparticles. All experiments were performed three times.

In vitro *photothermal effects on melanoma cancer cells*

Photothermal cancer therapy is a prospective approach for localized cancer treatment. In this paper, we used SiO_2@AuNPs absorbed in the DMEM supplemented with 10% fetal bovine serum, 1% of penesterep. The cells were incubated at 37 °C for 24 h. The culture medium was replaced with 100 μl of culture media containing 50 μg/ml FA-SiO_2@AuNPs for 4 h at 37 °C. SiO_2@AuNPs and FA-SiO_2@AuNPs were suspended in DMEM 10%. Cells were rinsed 3 times by PBS. Then, fresh culture medium was added to the wells. After exposing cells to laser pulses (808 nm wavelength, power density of 0.9 wcm^{-2}) for different irradiation times (30 s, 1, 2, 3, 4, 5, 6 and 7 min). Then, it was returned to the 37 °C incubator overnight. Following incubation, MTT assays were performed as previously described. The experiments were performed in triplicate.

Evaluation of cell apoptosis

A375 cells (1×10^4 cells/well) were seeded in 48-well plates and were incubated at 37 °C in a 5% CO_2 incubator for 24 h. Cells were treated with FA-SiO_2@AuNPs nanoparticle (50 μg/ml) for 4 h. The cells were washed by 100 μl of PBS, were trypsinized and were centrifuged. According to the manufacturers' instruction, the collected cells were re-suspended in binding buffer and were stained with 10 μl of Annexin V-FITC and PI for 15 min in the dark. Then, apoptosis was detected by BD FACS Caliber flow cytometer. The tests were carried out in triplicate.

Statistical analysis

Multigroup comparisons of the means were carried out by one-away ANOVA. Statistical significance for cell toxicity was set at $P < .05$. Results were expressed as mean ± SD ($n = 3$).

Results

Characterization of FA-SiO_2@AuNPs

The nanoparticle was synthesized as described in the synthesis section. In order to determine nanoparticles' distribution size and morphology of the nanoparticle, scanning electron microscopy (SEM) was performed. As shown in Figure 2, SEM images showed that the prepared nanoparticle is spherical in shape and has a uniform core/shell structure. The size distribution of the synthesized nanoparticle was also assessed using dynamic light scattering (DLS). According to Figure 3, the diameter of the synthesized nanoparticle is ~73.7 nm.

UV-visible spectroscopy is a method in which absorbed light measured by gold nanoparticles. The peaks of absorption in the UV-visible spectrum are dependent on the shape, size, and composition of gold nanoparticles [33]. The UV–Vis absorption spectra of the nanoparticle are shown in Figure 4. As shown in this figure, FA-SiO_2@AuNPs has higher NIR absorption, which is about 808 nm.

Fourier transform infrared (FTIR) spectroscopy is an analytical technique identifying chemical bonds and agent groups in gold nanoparticles through producing an infrared absorption spectrum. According to Figure 5, FTIR confirms the connection between the linker and Folic acid on the surface of SiO_2@Au within the region of 400–4000 cm^{-1}. In the study, FTIR for SiO_2@Au@Cys the bands at 3382.05 and 1610 cm^{-1} are assigned to stretching and bending vibration of OH groups respectively, due to the presence of OH groups of Cysteine. An increase in- intensity of OH peaks was observed in Folate-SiO_2@Au@Cys compared toSiO_2@Au@Cys. The peak at 1700 cm^{-1} is attributed to Carbonyl stretching vibration of amide and acidic groups. The aromatic out-of-plane ring stretching vibration and benzoic vibration in the folic acid molecule were observed at 1610 and 1515 cm^{-1}, respectively [34].

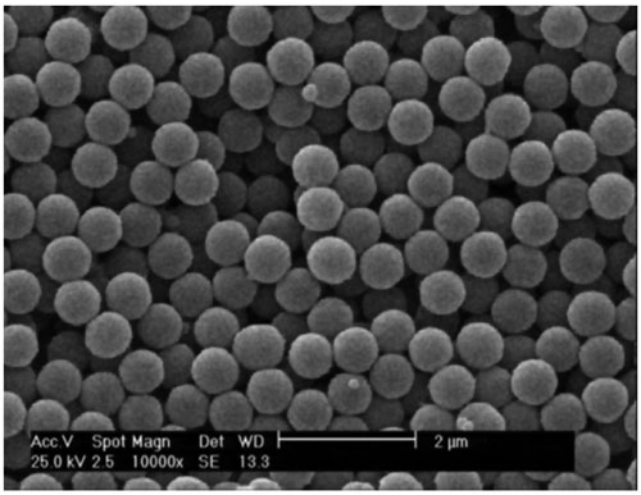

Figure 2. SEM images of SiO_2@Au core/shell nanoparticles.

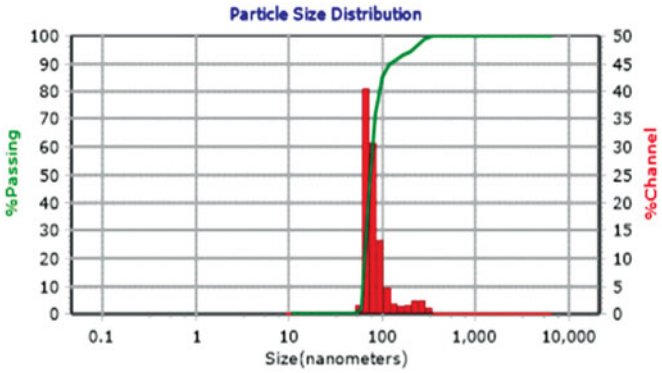

Figure 3. DLS measurement of size distribution of FA-SiO_2@AuNPs.

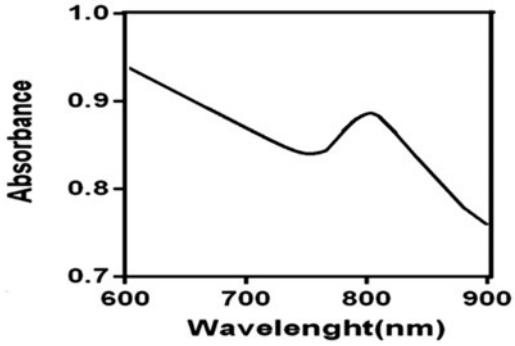

Figure 4. UV visible spectrum of FA-SiO_2@AuNPs.

Intra-cellular uptake of folate gold nanoshell into cancer cells

Figure 6 shows the affinity of cancer cells to the FA-SiO_2@AuNPs compared to the SiO_2@AuNPs, where the percentage of SiO_2@AuNPs and FA-SiO_2@AuNPs in cells was equal to 23.44% and 67.7%, respectively. In order to assess the "*in vitro*" capability of the FA-SiO_2@AuNPs in discriminating cancer cells from normal cells, an ICP-mass analysis was carried out on A375 and HDF cell lines. Figure 6 shows that FA-SiO_2@AuNPs intra-cellular uptake in A375 was equal to 67.7% which is higher than that which was found in HDF cell (2%).

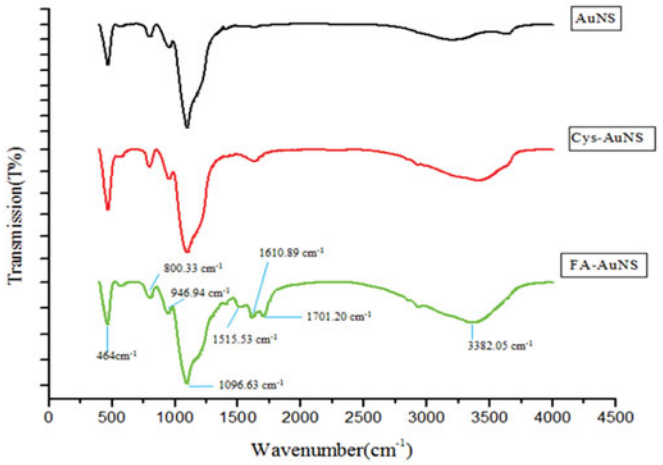

Figure 5. FTIR spectra of Folic acid conjugated withSiO_2@Au core-shell nanoparticles.

Results of cell viability (MTT) assay

MTT assays were performed using A375 and HDF cell lines to determine whether SiO_2@Au and FA-SiO_2@AuNPs have a toxic effect on A375 and HDF cell lines. MTT assay indicated (Figure 7), that the cell viability was set 100% as the control without nanoparticle treatment. MTT results showed that SiO_2@Au and FA-SiO_2@AuNPs treating on HDF cell were considered as nontoxic nanoparticles to a concentration of 100 µg/ml but FA-SiO_2@AuNPs treating on A375 cell was observed as significant toxicity at all concentration (untreated A375 and HDF cells were used as controls). No significant difference was observed between the toxicity of SiO_2@Au and FA-SiO_2@AuNPs on HDF (normal cell). However, there was an acceptable reduction in cell viability in higher concentrations. According to overexpression of folate receptors on the surface of cancerous cells, they are more sensitive to FA-SiO_2@AuNPs on A375 (cancer cell) at all concentration. It suggests that it may be applied as a targeting agent. FA-SiO_2@AuNPs is new preclinical therapeutic agent for melanoma cancer cells therapy which needs further investigation regarding using in animal models for applying in a human study in the future.

Results of in vitro photothermal effects on melanoma cancer cells

Results showed clearly, that gold Nanoshells could generate sufficient heat under near-infrared laser irradiation, which leads to localized cytotoxicity of cancer cells. The gold Nanoshells could ablate cancer cells through the PTT effect induced by the 808 nm laser irradiation. According to Figure 8, 808 nm and 4 min irradiation time exposure and a power density of 0.9 Wcm^{-2} were chosen for the PTT study. In addition, significant PTT toxicity was observed ($P < .05$). In addition, the cells untreated by laser irradiation, showed negligible cell death to about 25%. The data (Figure 8) indicated that, under NIR irradiation, SiO_2@AuNPs reduced the cell viability of A375 cells to about 48%. Cell viability compared to two groups of SiO_2@Au and FA-SiO_2@AuNPs reduced after photothermal therapy (31%, 16% of cell viability respectively).

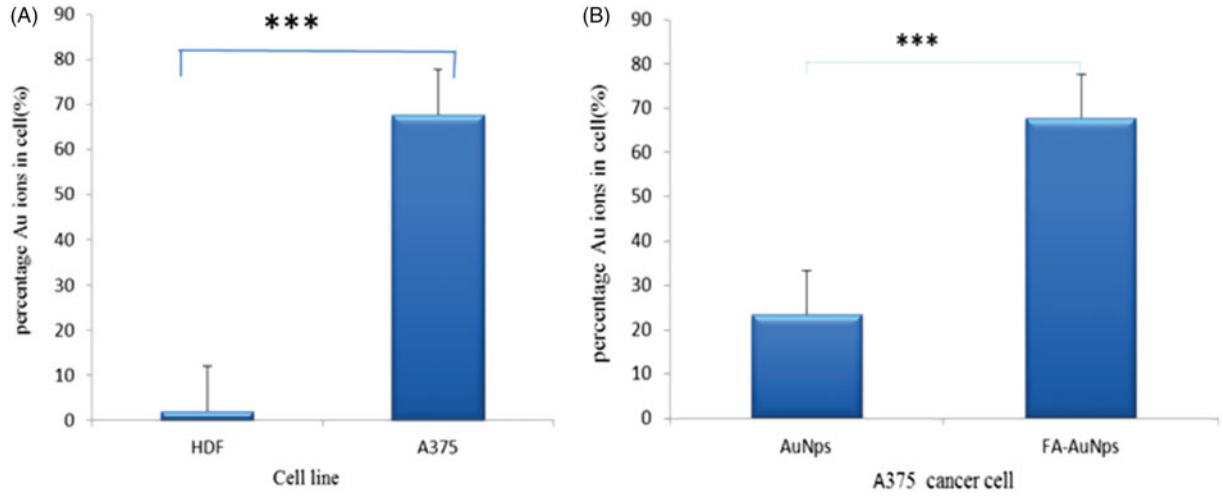

Figure 6. Intra-cellular uptake assay of SiO_2@Au and FA-SiO_2@AuNPs (A, B). (A) Comparison of the uptake of SiO2@Au and FA-SiO_2@AuNPs in A375 cancer cells. (B) Difference between the uptake of FA-SiO_2@AuNPs in HDF and A375 cell lines.

Considering the details, FA-SiO_2@AuNPs induced more cell death dramatically. These results suggest that the photothermal damaging effect of the SiO_2@AuNPs could be improved by folate targeting in A375 cells. Therefore, FA-SiO_2@AuNPs can be effective and can be considered as promising nanoparticles for PTT in folate receptor overexpressing in the cancer cell.

Results of cell apoptosis assay

The apoptosis percentages of A375 cells after the various treatments are shown in Figure 9. As can be seen in this figure, 3.82% and 5.89% of the cells were experienced apoptosis respectively in the untreated cell and under NIR laser irradiation after incubating, untreated cells. After exposing cells to SiO_2@Au, FA-SiO_2@Au NPs and laser irradiation in presence of SiO_2@Au and FA-SiO_2@Au NPs, the percentages of apoptotic cells increased about 21.16%, 23.82%, and 28.32%, 32.2%, respectively, Compared to the control group which was equal to 4%. There was a statistically significant difference between treated and untreated cells ($P < .05$). However, cells treated by laser combined with SiO_2@Au, FA-SiO_2@Au nanoparticles showed more apoptotic (28.32%, 32.2%, respectively) significantly ($P < .05$) than the other groups. These results indicated the apoptotic effects of nanoparticles. While the incidence of necrosis in all groups was observed to be average at 3%, it can be observed that these nanoparticles conduct cell death through the apoptosis pathway much more than necrosis. (the death in treated cells induced by nanoparticles and laser leads to cell death which is caused through apoptosis much more than necrosis). Definitely, this is considered as a significant privilege regarding these nanoparticles [35].

Discussion

In the present study, FA-SiO_2@Au nanoparticles were designed and synthesized as a new therapeutic agent for melanoma cancer cells therapy. The synthesized nanoparticle was assessed by various characterization methods. As shown in Figures 2 and 3, the synthesized FA-SiO_2@AuNPs is spherical in shape and the size of nanoparticles is about 73.7 nm. Optical absorption profile of FA-SiO_2@AuNPs was characterized by UV–visible spectroscopy (Figure 4), showing that nanoparticle has an appropriate absorption in NIR region. According to Figure 5, FTIR spectroscopy confirmed Cysteine as a linker and folic acid has been attached to SiO_2@Au successfully.

Based on the results of ICP-mass, as shown in Figure 6, the A375 cells demonstrated higher uptake more than 23 times using FA-SiO_2@AuNPs than that of the HDF cells after 2 h of incubation. In addition, the A375 cells demonstrated uptake which was ~2 times using FA-SiO_2@AuNPs than that of SiO_2@AuNPs. This might be due to the more metabolic activity of A375 cells leading to the overexpression of the folate receptors on the surface of the cancerous cell and the low metabolic activity of HDF cells.

In this study, the cytotoxic effects of gold Nanoshell were investigated on HDF and A375 cells. Different concentrations of gold Nanoshell were used with and without conjugation to folic acid. NIR laser with wavelength of 808 nm and power density of 0.9wcm^{-2} was applied as the heating source. The cytotoxicity of the nanoparticles was determined firstly by evaluating the viability of normal and cancer cells (HDF and A375) using an MTT assay. The results indicated that the concentration of 50 μg/ml of FA-SiO_2@AuNPs and incubation time of 4 h in cancer cells increases cell death after being exposed to NIR irradiation. So that the viability of cancer cells in present FA-SiO_2@AuNPs reduced compared to SiO_2@AuNPs by 31%, also the viability of A375 cells in this concentration compared to normal cells reduced by 27%. Therefore, at a concentration of the nanoparticles (50 μg/ml), HDF cells presented high cell viability, which suggested that the nanoparticle had low cytotoxicity on HDF cells, but the nanoparticles did induce a high level of toxicity in A375 cell at a concentration of 50 μg/ml (Figure 7). Therefore, these results can be considered as an advantage regarding using

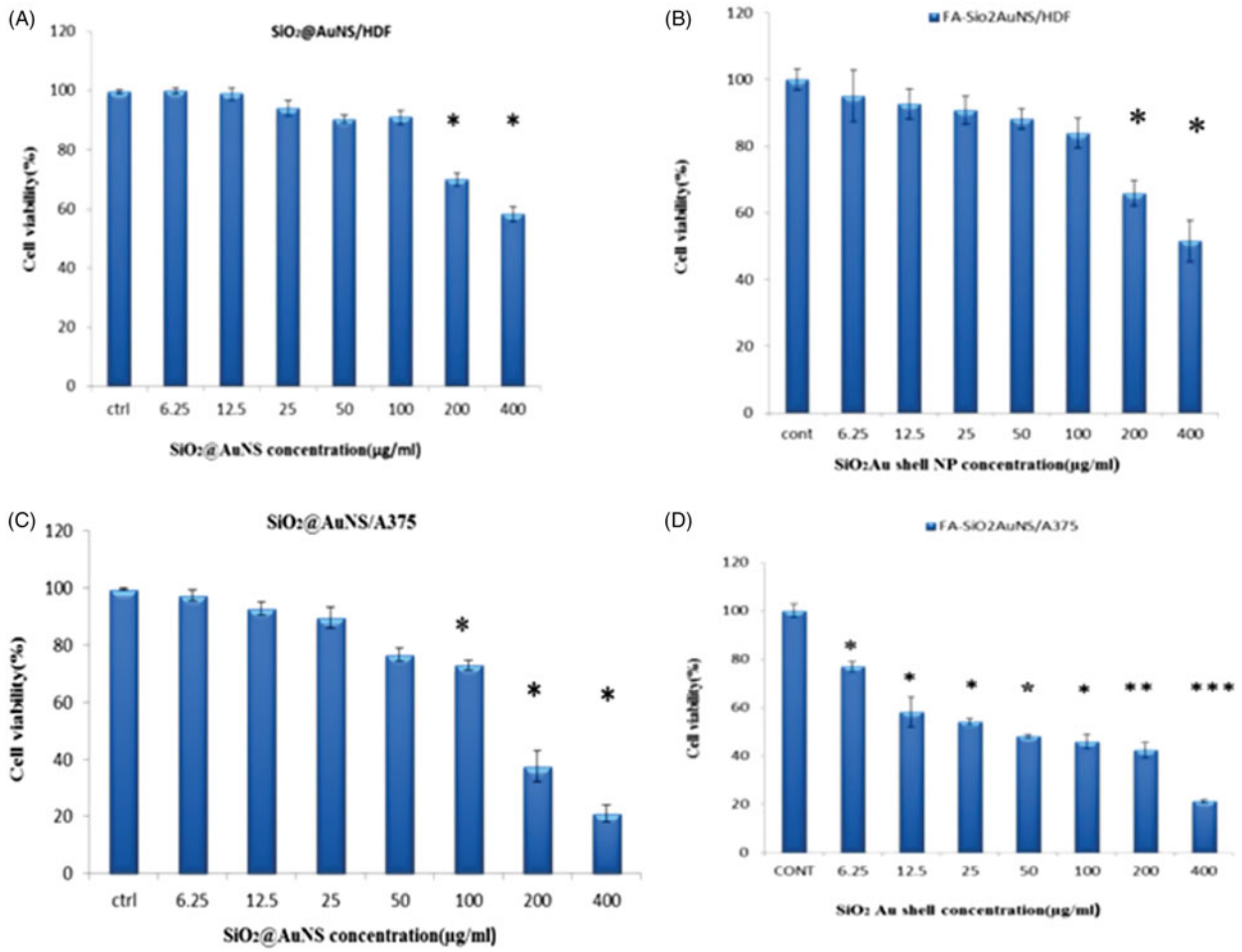

Figure 7. Cytotoxicity of SiO_2@Au and FA-SiO_2@AuNPs in A375 and HDF cell lines. The cells were incubated using different concentrations of NPs in the range from 6.25 μg/ml to 400 μg/ml for a time period of 24 h (mean ± standard deviation; $n = 3$).
Abbreviations: cytotoxicity of A (SiO_2@Au in HDF cell line); B (FA-SiO_2@AuNPs in HDF cell line); C(SiO_2@Au in A375 cell line); D(FA-SiO_2@AuNPs in A375 cell line). Notes: $^*P < .05$; $^{**}P < .01$; $^{***}P < .001$.

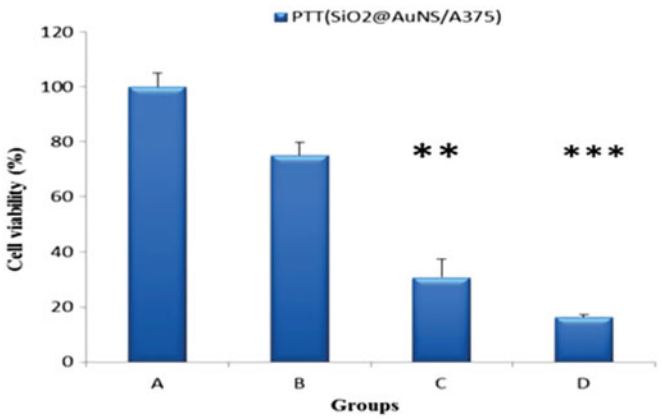

Figure 8. The photo toxicity of SiO_2@Au and FA-SiO_2@AuNps in A375 cell with and without laser irradiation. Untreated control cells, treated cells by laser alone, Treated cells by Laser combined with SiO_2@Au nanoparticles, Treated cells by Laser combined with FA-SiO_2@Au nanoparticles. The cells were incubated using 50 μg/ml concentration of NPs. Cell viability data obtained from the MTT assay of A375 cells after various treatments groups without and with irradiation by the 808 nm laser for 4 min. Notes: $^*P < .05$; $^{**}P < .01$; $^{***}P < .001$.

these nanoparticles in the treatment of melanoma cancer cell line A375.

The effects of photothermal therapy using the synthesized nanoparticles were also evaluated by MTT assay and flow cytometry. It was demonstrated that the ability of FA-SiO_2@AuNPs caused selective death in cancer cells (A375) with highly overexpressed folate receptors under a NIR laser irradiation (Figure 8). This selective effect decreased, due to conjugation of folic acid to nanoparticles, also at 50 μg/ml concentration of the nanoparticles, the time of laser NIR irradiation on A375 cell, and by reducing the duration of NIR radiation, the side effects of the laser also diminished. MTT assay showed that considering cell viability under the laser NIR radiation without being exposed to nanoparticles in cancer cells up to 4 min was not significantly different compared to the control group. However, at times which were more than 4 min (5, 6, and 7 min) the viability of cells decreased to about 38%, 13% and 7%, respectively. So the time of 4 min and 50 μg/ml of concentration were chosen as the best time of laser NIR irradiation and the effective concentration of nanoparticles. Therefore, FA-SiO_2@AuNPs was as an active targeting agent for photothermal therapy with more than 80% of A375 cells death after NIR laser irradiation. In addition, it was found that the majority of cell deaths was related to the apoptosis process (Figure 9).

These results are consistent with the results of other studies demonstrated by other researchers. Mehdizadeh et al. conducted a study on the photothermal effects of folic acid

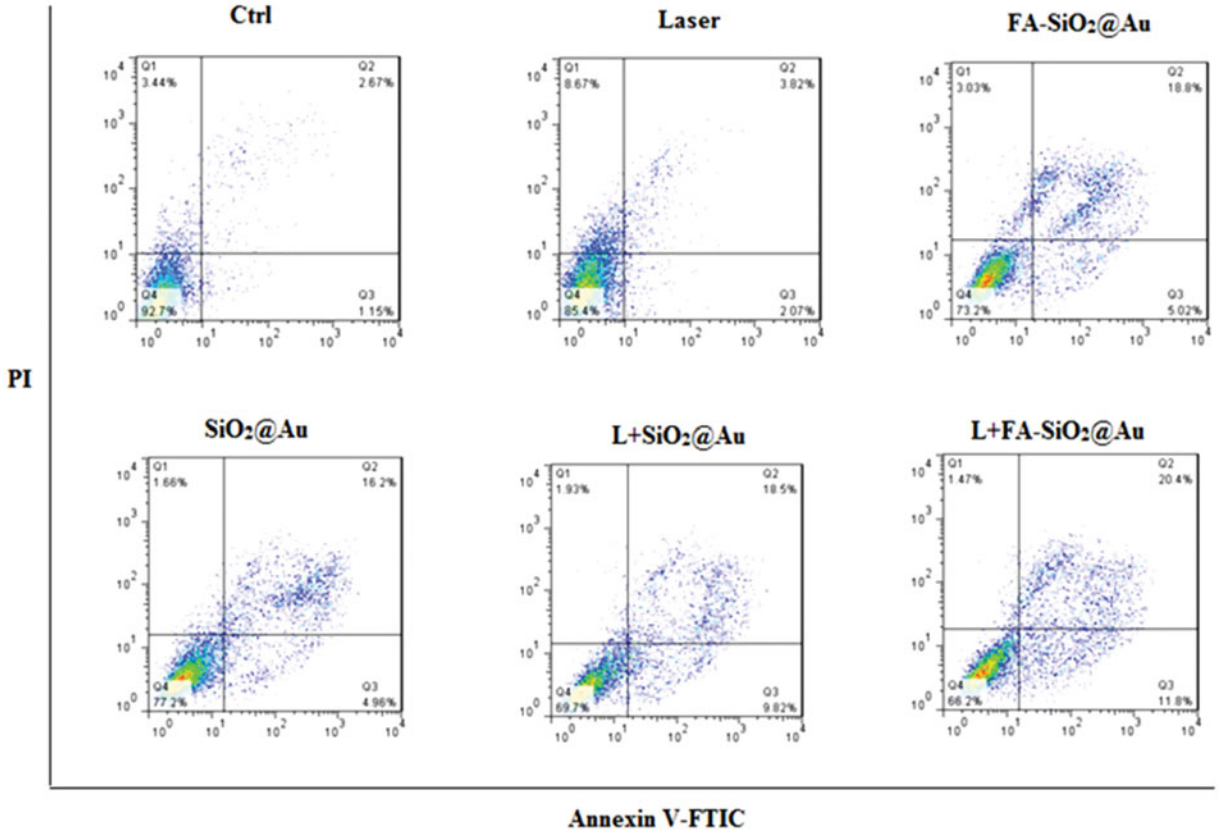

Figure 9. FITC-labeled Annexin V apoptosis assay in the FR-positive A375 cells. (A) Untreated control cells, (B) Treated cells by laser alone, (C) Treated cells by FA-SiO_2@Au nanoparticles, (D) Treated cells by SiO_2@Au nanoparticles, (E) Treated cells by Laser combined with SiO_2@Au nanoparticles, (F) Treated cells by Laser combined FA- SiO_2@Au nanoparticles. Abbreviations: Q1: necrosis cells; Q2: late apoptosis cells; Q3: early apoptosis cells; Q4: live cell.

conjugated gold Nanorods (FA-AuNRs) on human nasopharyngeal carcinoma cell line KB. They indicated that under treatment by laser irradiation (755 nm; 40J/cm^2; 7 pulses; pulse duration: 3 min) or using FA-AuNRs alone, no cytotoxicity was observed. Whereas using combined plasmonic photothermal therapy with 20 μM of FA-AuNRs, the 56% of cell death was observed for KB cells [36].

In the field of multifunctional nanoparticles, photothermal effects of gold Nanoshell functionalized with anti-HER2 were studied by Naomi Halas et al. as a targeting agent designed for photothermal therapy of SKBr3 breast cancer cells. They synthesized immune targeted Nanoshells to both scatter light in the NIR enabling optical imaging of molecular cancer and to absorb light. They reported that immune targeted Nanoshells are used to detect and kill breast carcinoma cells that overexpress the HER2, as a relevant cancer biomarker and selective ablation of targeted cancer cells through photothermal therapy. Cells were exposed to NIR irradiation (820 nm, 0.08 W/m^2 for 7 min). After photothermal therapy, cell death was observed only in cells treated by NIR laser following being exposure to anti-HER2 Nanoshells. This effect was not observed in cells treated either by Nanoshells conjugated to a nonspecific antibody or by NIR light alone [37].

In another study conducted by Habib Ghaznavi et al, the folate-conjugated PEG-coated Au@IONP core-shell Nano complex was synthesized and The photothermal effects of Nano complex on both KB and MCF-7 (human breast adenocarcinoma) cell lines were investigated. The cytotoxicity of the Nano complex was determined by MTT assay and flow cytometry. Significant cell death was observed for KB (62%) and MCF-7 (33%) cells following photothermal therapy. Results indicated that KB cells overexpress folate receptors on their membrane but MCF-7 has a lower level of folate receptor expression [22].

In another study conducted by Da-Wi Wang et al, the effects of photothermal therapy super-paramagnetic iron oxide (SPIO) core and gold Nanorod (GNRs) by laser NIR irradiation on cancer cells was investigated and it was observed that the Fe_3O_4@SiO_2@GNRs-FA nanoparticles had more uptake in KB cells compared to Fe_3O_4@SiO_2@GNRs nanoparticles and viability of cells decreased to more than 50% after being exposed to laser radiation [11]. Thus, results showed that the Fe_3O_4@SiO_2@GNRs-FA is an effective photothermal therapy agent in terms of folate-receptor overexpressing in cancer cells, which is in accordance with the results obtained in this study.

These promising *in vitro* results indicate that the FA-SiO_2@Au nanoparticles can generate sufficient heat under near-infrared irradiation to cause the cytotoxicity of cancer cells. Although, the results of the *in vitro* study, which were reported here, have demonstrated some important steps

successfully regarding the FA-SiO_2@Au nanoparticles combined with photothermal therapy. Translation of this modality to animal experiments is required clearly.

Conclusions

In this study, a SiO_2@Au nanoparticle was engineered successfully for use in cancer therapy. The prepared nanoparticle was functionalized with folic acid to target the cancer cells which overexpress folate receptors on their surfaces. It was demonstrated that FA-SiO_2@Au nanoparticles could be used as an effective photothermal therapeutic agent for folate-receptor overexpressing in melanoma cancer cell line A375. This new therapeutic method for cancer therapy suggests further investigation in terms of using *in vivo* models for application in humans.

Acknowledgements

This study was adapted from an MSc thesis written by Fateme Sadat Majidi. We thank Davoodabadi sincerely for providing the laser device and the bodies (Sara Mayahi, Zahra Balavandi) who helped us in the project.

Disclosure statement

No potential conflict of interest was reported by the authors.

Funding

We acknowledge the financial support provided by the Research Council of Iran University of Medical Science.

References

[1] Markovic SN, Erickson LA, Rao RD, et al. Malignant melanoma in the 21st century, part 1: epidemiology, risk factors, screening, prevention, and diagnosis. Mayo Clin Proc. 2007;82:364–380.
[2] Tsao H, Sober AJ. Melanoma Treatment Update,. Dermatol Clin. 2005;23:323–333.
[3] Jemal A, Siegel R, Xu J, et al. Cancer Statistics, 2010 both sexes female both sexes estimated deaths. CA Cancer J Clin. 2010;60:277–300.
[4] Miller KD, Siegel RL, Lin CC, et al. Cancer treatment and survivorship statistics, 2016. CA Cancer J Clin. 2016;66:271–289.
[5] Lopez-graniel CM, Ochoa-carrillo FJ, Meneses-garcõâa A. Malignant melanoma of the oral cavity: diagnosis and treatment experience in a Mexican population. Oral Oncol. 1999;35:425–430.
[6] Vikey AK, Vikey D. Primary malignant melanoma, of head and neck: a comprehensive review of literature. Oral Oncol. 2012;48:399–403.
[7] Bhatia S, Tykodi SS, Thompson JA.Treatment of metastatic melanoma: an overview. Oncology (Williston Park) 2009;23:488–496.
[8] Hehr T, Wust P, Bamberg M, et al. Current and potential role of thermoradiotherapy for solid tumours. 2003;26:295–302.
[9] Ferrari M. Cancer nanotechnology: opportunities and challenges. Nat Rev Cancer. 2005;5:161–171.
[10] Peer D, Karp JM, Hong S, et al. Nanocarriers as an emerging platform for cancer therapy. Nat Nanotechnol. 2007;2:751–760.
[11] Wang D-W, Zhu X-M, Lee S-F, et al. Folate-conjugated Fe_3O_4@SiO_2@gold nanorods@mesoporous SiO_2 hybrid nanomaterial: a theranostic agent for magnetic resonance imaging and photothermal therapy. J Mater Chem B. 2013;1:2934–2942.
[12] Madsen SJ, Shih E, Christie C, et al. Photothermal enhancement of chemotherapy mediated by gold-silica nanoshell-loaded macrophages: in vitro squamous cell carcinoma study. J of Biomedical Optics. 2016;21:018004.
[13] Kumaradas JC, Sherar MD. An edge-element based finite element model of microwave heating in hyperthermia: method and verification. Int J Hypertherm. 2002;18:426.
[14] Ohguri T, Imada H, Kato F, et al. Radiotherapy with 8 MHz radiofrequency-capacitive regional hyperthermia for pain relief of unresectable and recurrent colorectal cancer. Int J Hypertherm. 2006;22:1–14.
[15] Arthur RM, Straube WL, Trobaugh JW, et al. Non-invasive estimation of hyperthermia temperatures with ultrasound. Int J Hyperther. 2005;21:589–600.
[16] Horisberger M, Tacchini-Vonlanthen M. Ultrastructural localization of Kunitz inhibitor on thin sections of glycine max (Soybean) cv. maple arrow by the gold method. Histochem. 1983;77:37–50.
[17] Jain S, Hirst DG, O'Sullivan JM. Gold nanoparticles as novel agents for cancer therapy. The Brit J Radiol. 2012;85:101–113.
[18] Sau TK, Murphy CJ, Commun MLHC, et al. Seeded high yield synthesis of short Au nanorods in aqueous solution. Langmuir. 2004;20:6414–6420.
[19] Zhang J, Langille MR, Personick ML, et al. Concave cubic gold nanocrystals with high-index facets. JACS. 2010;132:14012–14014.
[20] Hainfeld JF, Connor MJO, Lin P, et al. Infrared-transparent gold nanoparticles converted by tumors to infrared absorbers cure tumors in mice by photothermal therapy. PLOS One. 2014;9:e88414.
[21] Eyvazzadeh N, Shakeri-zadeh A, Fekrazad R, et al. Gold-coated magnetic nanoparticle as a nanotheranostic agent for magnetic resonance imaging and photothermal therapy of cancer. Lasers in Med Sci. 2017;32:1469–1477.
[22] Journal AI, Ghaznavi H, Hosseini-nami S, et al. Folic acid conjugated PEG coated gold – iron oxide core – shell nanocomplex as a potential agent for targeted photothermal therapy of cancer. Artif Cells Nanomedicine Biotechnol. 2017;0:1–11.
[23] Mansoori GA, Brandenburg KS, Shakeri-zadeh A. A comparative study of two folate-conjugated gold nanoparticles for cancer nanotechnology applications. Cancers 2010;7:1911–1928.
[24] Mayle KM, Dern KR, Wong VK, et al. Polypeptide-based gold nanoshells for photothermal therapy. SLAS Tech. 2017;22:18–25.
[25] Huang X, Qian W, El-sayed IH, et al. The potential use of the enhanced nonlinear properties of gold nanospheres in photothermal cancer therapy. 2007;753:747–753.
[26] Ansorge W, Pepperkok R. Performance of an automated system for capillary microinjection into living cells. J Biochem Biophys Meth. 1988;16:283–292.
[27] Li L, Gao F, Jiang W, et al. Folic acid-conjugated superparamagnetic iron oxide nanoparticles for tumor-targeting MR imaging. Drug Deliv. 2015;00:1–8.
[28] Sudimack J, Lee RJ. Targeted drug delivery via the folate receptor. Adv Drug Deliv Rev. 2000;41:147–162.
[29] Lee JY, Park JH, Kim SW. Synthesis and evaluation of folate-immobilized 198Au@SiO2 nanocomposite materials for the diagnosis of folate-receptor- overexpressed tumor. Bull Kor Chem Soc. 2016;37:219–225.
[30] Doucette MM, Stevens VL. Folate receptor function is regulated in response to different cellular growth rates in cultured mammalian cells. J Nutri. 2001;131:2819–2825.
[31] Choma J, Dziura A, Jamioła D, et al. Preparation and properties of silica – gold core – shell particles. Coll Surf A: Physicochem Eng Asp. 2011;373:167–171.
[32] Phonthammachai N, Kah JCY, Jun G, et al. Synthesis of contiguous silica - gold core - shell structures: critical parameters and processes. Langmuir 2008;24:5109–5112.

[33] Owen AE. Fundamentals of UV-visible spectroscopy. Germany: Hewlett-Packard; 1996.
[34] Berthomieu C, Hienerwadel AER. Fourier transform infrared (FTIR) spectroscopy. Photosynth Res. 2009;101:157–170.
[35] Manuscript A, Society R, Manuscripts A, et al. Cellular uptake, imaging and pathotoxicological studies of novel Gd [III]-DO3A-butrol Nano-Formulation.
[36] Mehdizadeh A, Pandesh S, Shakeri-zadeh A, et al. The effects of folate-conjugated gold nanorods in combination with plasmonic photothermal therapy on mouth epidermal carcinoma cells. Lasers in Med Sci. 2013;29:939–948.
[37] Loo C, Lowery A, Halas N, et al. Immunotargeted nanoshells for integrated cancer imaging and therapy. Nano Lett. 2005;5:709–11.